

Observation of Spatial Quantum Correlations Induced by Multiple Scattering of Nonclassical Light

S. Smolka,^{1,*} A. Huck,² U. L. Andersen,² A. Lagendijk,³ and P. Lodahl^{1,†}

¹*DTU Fotonik, Department of Photonics Engineering, Technical University of Denmark, Building 345V, 2800 Kongens Lyngby, Denmark*

²*DTU Physics, Department of Physics, Technical University of Denmark, Building 309, 2800 Kongens Lyngby, Denmark*

³*FOM Institute for Atomic and Molecular Physics, Kruislaan 407, 1098 SJ Amsterdam, The Netherlands*

(Received 21 November 2008; published 13 May 2009)

We present the experimental realization of spatial quantum correlations of photons that are induced by multiple scattering of squeezed light. The quantum correlation relates photons propagating along two different light paths through the random medium and is infinite in range. Both positive and negative spatial quantum correlations are observed when varying the quantum state incident to the multiple scattering medium, and the strength of the correlations is controlled by the number of photons. The experimental results are in excellent agreement with recent theoretical proposals by implementing the full quantum model of multiple scattering.

DOI: 10.1103/PhysRevLett.102.193901

PACS numbers: 42.25.Dd, 42.50.Lc, 78.67.-n

Multiple scattering of light waves propagating through a disordered medium can be described as a random walk of the direction of propagation whereby the medium becomes opaque [1]. Such multiple scattering determines the performance of nanophotonic devices based on, e.g., photonic crystals [2] or surface plasmon polaritons [3] and can be applied for enhancing the information capacity for optical communication [4]. In multiple scattering, the different possible light paths through the random medium will interfere, and a complex spatial intensity distribution of light is generated; cf. Fig. 2(b). Usually, interference effects tend to vanish after averaging over all possible realizations of the disorder, and the light transport is described by diffusion theory. Under conditions where multiple scattering is strong, light diffusion is modified leading to mesoscopic fluctuations and spatial correlations [1,5,6]. These correlations imply that the light intensity observed at one position after the medium depends on the intensity at a different position even after averaging over all ensembles of disorder.

The significance of the quantum nature of light in a multiple scattering context has been addressed only recently [7–13]. Pioneering work has provided the theoretical framework for a quantum optical description of multiple scattering [7] that was used to predict the existence of spatial quantum correlations induced by multiple scattering of nonclassical light [9]. These quantum correlations exist even in the diffusive regime of multiple scattering and add to the traditional mesoscopic correlations that are of classical origin [1]. Here we present the experimental demonstration of spatial quantum correlations induced by multiple scattering of squeezed light.

Because of the Heisenberg uncertainty principle, intrinsic quantum fluctuations are always present. Although always of inherent quantum origin, photon fluctuations are

classified as either classical or nonclassical if similar fluctuations can be induced by classical light sources or not. The classical boundary corresponds to Poissonian photon statistics where the variance of the photon number fluctuations equals the mean number of photons. A purely quantum regime exists where photon fluctuations are reduced beyond the classical limit leading to sub-Poissonian photon statistics.

The number of photons exiting a multiple scattering medium in a specific direction can be correlated or anti-correlated with the number of photons in another direction, and this spatial correlation depends on the quantum state of light illuminating the medium. The degree of correlation is quantified by the spatial quantum correlation function [14]

$$\overline{C_{abab}^Q} = \frac{\overline{\langle \hat{n}_{ab} \hat{n}_{ab'} \rangle}}{\overline{\langle \hat{n}_{ab} \rangle} \overline{\langle \hat{n}_{ab'} \rangle}}, \quad (1)$$

where a labels the direction of the incident light and b and b' the two different output directions. The operator \hat{n}_{ab} represents the number of photons in output mode b . $\langle \dots \rangle$ denotes the quantum mechanical expectation value, while the bars refer to an average over all realizations of disorder. The need for two averages is due to the fact that quantum fluctuations and random multiple scattering are both stochastic processes. $\overline{C_{abab}^Q}$ is the quantum optical generalization of the classical intensity correlation function that has been intensely investigated in multiple scattering experiments [1]. Note that the quantum correlations are induced by a multiple scattering medium with a fully linear response. Thus, a nonclassical resource combined with linear optics is quite generally sufficient for many quantum optics experiments and even enables quantum computing [15].

The spatial quantum correlation function defined in Eq. (1) depends sensitively on the number and fluctuations of photons incident on the sample through direction a . By restricting to a theory for discrete spatial and temporal degrees of freedom, it is given by

$$\overline{C_{abab'}^Q} = \left[1 + \frac{F_a - 1}{\langle \hat{n}_a \rangle} \right] \left[1 + \overline{C_{abab'}^{(2)}} + \overline{C_{abab'}^{(3)}} \right]. \quad (2)$$

$\langle \hat{n}_a \rangle$ is the average number of incident photons, and the Fano factor $F_a = \Delta n_a^2 / \langle \hat{n}_a \rangle$ gauges the variance in the photon number fluctuations specified within the spectral bandwidth relevant for the measurement. $\overline{C^{(2)}}$ and $\overline{C^{(3)}}$ are classical spatial correlation functions [1] that can be neglected in the diffusive regime of multiple scattering that is of concern here, but it would certainly be exciting to study their quantum optical equivalents as well [11]. The size of the Fano factor determines the transition from the classical ($F_a \geq 1$) to the nonclassical regime ($F_a < 1$). Using nonclassical light opens the door to a genuine quantum regime where $0 \leq C_{abab'}^Q < 1$, corresponding to spatially anticorrelated photons. Such spatial quantum correlations are of *infinite range* in the sense that the magnitude is independent of the angular difference of the two output directions, which translates into a spatial separation in the far field. This is an example of the fundamentally new phenomena that arise in quantum optical descriptions of multiple light scattering. So far, quantum optical variables have been measured in very few multiple scattering experiments that have focused only on the regime of classical photon fluctuations [10,11], while spatial quantum correlations were not demonstrated.

The spatial quantum correlation function of Eq. (1) can be obtained by recording the photon fluctuations of the total transmission Δn_T^2 and total reflection Δn_R^2 , respectively. They are related through [9]

$$\frac{\Delta n_T^2}{\langle \hat{n}_a \rangle} = \eta \frac{\ell}{L} + \langle \hat{n}_a \rangle \eta^2 \left(\frac{\ell}{L} \right)^2 \left(\overline{C_{abab'}^Q} - 1 \right), \quad (3a)$$

$$\frac{\Delta n_R^2}{\langle \hat{n}_a \rangle} = \eta \left(1 - \frac{\ell}{L} \right) + \langle \hat{n}_a \rangle \eta^2 \left(1 - \frac{\ell}{L} \right)^2 \left(\overline{C_{abab'}^Q} - 1 \right), \quad (3b)$$

which holds in the diffusive regime of multiple scattering where the spatial correlation function is independent of the output direction b . The overall detection efficiency η expresses the fraction of transmitted or reflected light that is actually detected and should be large in order to observe quantum effects. We observe that the spatial quantum correlation function $\overline{C_{abab'}^Q}$ is directly accessible by measuring in addition to the photon fluctuations also the detection efficiency, the average number of photons entering the sample $\langle \hat{n}_a \rangle$, and the ratio of the transport mean free path to the sample thickness ℓ/L . Note that, when comparing to the experiment, the latter ratio represents the en-

semble averaged sample transmission coefficient that is influenced by extrapolation lengths to account for the effects of the interface of the multiple scattering medium [16]. In the experiment, we extract the spatial correlation function in the frequency domain, which has dimensions of an inverse bandwidth. The complete continuous mode theory will be described elsewhere [17].

As a nonclassical resource we use squeezed light generated in a second-order nonlinear process at a wavelength of $\lambda = 1064$ nm [18]. This versatile source features continuous tuning between classical (super-Poissonian) and nonclassical (sub-Poissonian) photon fluctuations by varying the relative phase between the squeezed vacuum state generated in the nonlinear process and a bright displacement beam. We are able to reduce photon fluctuations ($F_a = 0.52 \pm 0.02$) below the classical limit ($F_a = 1$) and induce excess fluctuations above the classical limit ($F_a = 4.6 \pm 0.2$). The multiple scattering experiment is conducted by focusing the nonclassical light source onto either the front surface or the back surface of the sample [cf. Fig. 1(a)] to perform total transmission and total reflection measurements, respectively. We record the total number of photons and the photon fluctuations transmitted

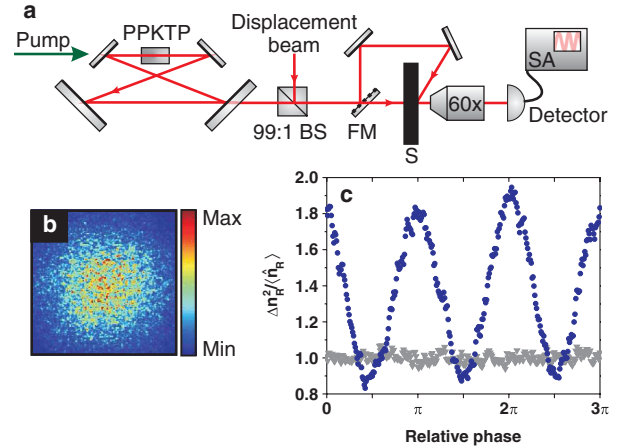


FIG. 1 (color online). (a) Sketch of the experimental setup. Vacuum squeezing is generated in an optical parametric oscillator with a periodically poled potassium titanyl phosphate (PPKTP) nonlinear crystal, overlapped with a displacement beam on a beam splitter (BS), and directed onto the sample (S). The flip mirror (FM) is used to choose between transmission and reflection measurements. The multiple scattered light is imaged onto a photodetector, and its photon fluctuations are recorded using an electronic spectrum analyzer (SA). (b) Measured spatial intensity distribution of light transmitted through a multiple scattering medium displaying a volume speckle pattern. (c) Measured photon fluctuations after multiple scattering recorded in reflection geometry ($L = 20 \mu\text{m}$). The photon fluctuations of the total reflection for a squeezed light source (blue circles) and the classical limit (gray triangles). Depending on the phase of a displacement beam, photon fluctuations below or above the classical limit are detected. The detection frequency was 3.93 MHz and the resolution bandwidth 300 kHz.

through or reflected from the sample. In the reflection geometry, the contributions from single-scattering events are avoided by illuminating the sample surface under a steep angle. The multiple scattering samples consist of TiO_2 that has been ground into strongly scattering particles with a typical size of 200 nm. A range of samples with different thicknesses has been fabricated. From total transmission measurements on each sample with an integrating sphere, both the detection efficiency and the transport mean free path can be extracted. The former is plotted in Fig. 2(c) and depends on sample thickness since the amount of light collected by the microscope objective in the experiment varies with sample thickness. The transport

mean free path is found to be $\ell = 0.9 \pm 0.3 \mu\text{m}$; i.e., all samples are in the diffusive regime where $\lambda/2\pi < \ell \ll L$. Note that the relatively large error bar on ℓ arises since the contribution from extrapolation lengths must be accounted for when deriving it from total transmission measurements [16]. The uncertainties in the experimental parameters entering the theory of Eqs. (3) lead to the shaded areas indicated in Figs. 2(a) and 2(b).

Figure 1(c) shows the measured photon fluctuations, recorded in reflection, for squeezed light illumination of the multiple scattering medium. The classical limit was recorded by blocking the squeezed beam. The phase of the displacement beam is scanned in order to continuously tune the photon fluctuations of the incident light below and above the classical limit. We record photon fluctuations that are reduced 0.5 ± 0.1 dB below the classical limit after the photons have been multiple scattered, which corresponds to a Fano factor for the total reflection of $F_R = 0.90 \pm 0.02$. Correcting for the detection efficiency of $(37 \pm 1)\%$, we infer $F_R = 0.72 \pm 0.04$ for light exiting the multiple scattering sample. The reduction of $F_R < 1$ is the direct experimental proof that nonclassical properties of light survive the complex stochastic process of multiple scattering even after ensemble averaging over realizations of disorder despite the common belief that quantum properties of light are fragile. We calculate the average number of scattering events in the multiple scattering process [19], which is given by $N \sim (L/\ell)^2$. For the particular sample used for the measurements of Fig. 1(c), we get $N \approx 1000$, when including effects of the interface [16], which quantifies the complexity of the multiple scattering process. We note that the reduction in the photon fluctuations shows that the information capacity associated with the multiple scattering channels can be enhanced beyond the classical limit, as predicted theoretically [8].

We have carried out a detailed investigation of the transport of nonclassical and classical photon fluctuations through the multiple scattering medium for a range of different sample thicknesses. Figures 2(a) and 2(b) display the detected photon fluctuations after multiple scattering plotted versus the sample thickness. Using light sources with classical fluctuations, the multiple scattered light always displays excess photon fluctuations corresponding to the classical regime [Fig. 2(a)]. Nonclassical light allows entering the quantum regime where the photon fluctuations are reduced below the classical limit; see Fig. 2(b). Our experimental results can be compared to the predictions from the full quantum theory for multiple scattering of photons [9,12]. Excellent agreement between experiment and theory is apparent from Fig. 2 in both the classical and the quantum regime. It should be stressed that the comparison to theory requires no adjustable parameters and depends only on measured parameters.

The theory predicts that the multiple scattered photon fluctuations depend on two terms varying as L^{-1} and L^{-2} , respectively; cf. Eqs. (3). The latter term is observable only for nonvanishing spatial quantum correlations; i.e., the

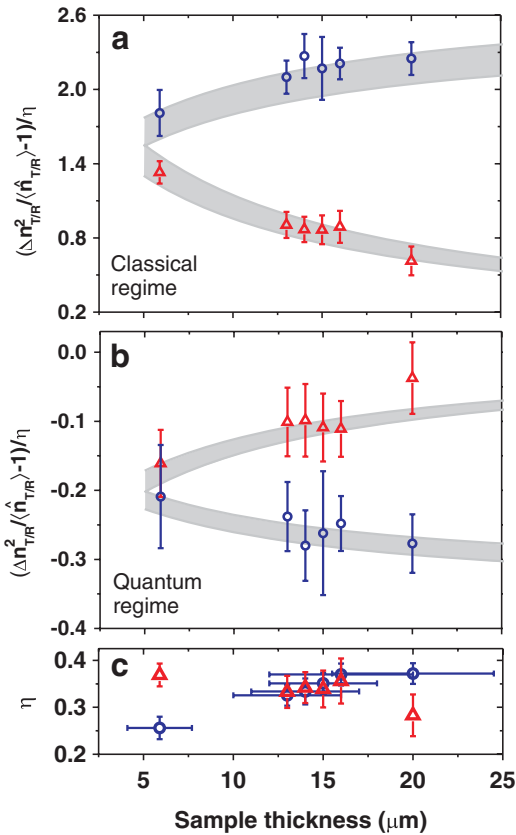


FIG. 2 (color online). Measured transmitted (red triangles) and reflected (blue circles) photon fluctuations scaled to η after multiple scattering of light with (a) classical ($F_a = 4.6$) and (b) nonclassical ($F_a = 0.52$) photon fluctuations versus sample thickness. The classical limit $(\Delta n_{T,R}^2 / \langle \hat{n}_{T,R} \rangle - 1) = 1$ marks the boundary between the classical regime and the quantum regime. Every data point is obtained after ensemble averaging over six different sample positions. The shaded areas correspond to the theoretical predictions and incorporate the uncertainties in F_a , ℓ , and the extrapolation lengths. (c) Separately measured overall detection efficiency η for each sample thickness in transmission (red triangles) and reflection geometry (blue circles). The error bars on the sample thicknesses are plotted only once and should be considered as upper boundaries since they were obtained by characterizing inhomogeneities of the whole sample rather than the small area used for optical characterization.

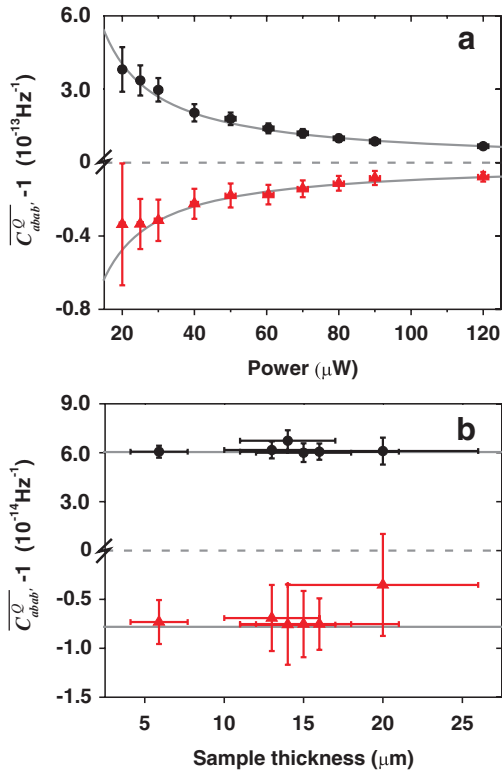


FIG. 3 (color online). (a) Measured spatial quantum correlation function C_{abab}^Q versus power of the incident light beam. For classical ($F_a = 4.6$, black points) and nonclassical ($F_a = 0.52$, red triangles) photon fluctuations, positive and negative spatial correlations are observed, respectively. Every data point represents an average over three different positions on the sample of thickness $L = 6 \mu\text{m}$. The curves are the theoretical predictions, and the dashed line represents the uncorrelated case. (b) Spatial quantum correlation function versus sample thickness taken at an input power of $P = 120 \mu\text{W}$. The spatial quantum correlation function is found to be independent of the sample thickness in agreement with theory (horizontal lines).

comparison between experiment and theory allows extracting the spatial quantum correlation function as explained above; cf. Fig. 3. We observe negative (positive) spatial correlations in the case where the transmitted photon fluctuations are in the quantum (classical) regime. According to Eq. (2), the strength of the spatial quantum correlation is expected to increase when reducing the number of photons of the incident light. This pronounced behavior is clearly demonstrated in Fig. 3(a) and is in excellent agreement with theory. Controlling the power of the nonclassical light source thus provides an efficient way of tuning the strength of the spatial quantum correlations. Furthermore, the spatial correlation function is predicted to be independent of the sample thickness, which holds in the diffusive regime of multiple scattering. This behavior is experimentally confirmed as well; see Fig. 3(b).

We presented the first experimental demonstration that photon fluctuations below the classical limit can be ob-

served after multiple scattering using squeezed light as a nonclassical resource. Multiple scattering was found to induce infinite range spatial correlations that are of a purely quantum origin. Our experimental results were in excellent agreement with the full quantum optics theory for multiple scattered light. We believe that our results will inspire further explorations of the multitude of new phenomena encoded in the quantum optical properties of multiple scattered light.

We thank Jirí Janousek for help with the nonclassical light source and Elbert G. van Putten, Ivo M. Vellekoop, and Allard P. Mosk for providing the samples. We gratefully acknowledge the Danish Research Agency for financial support (Project No. FNU 645-06-0503). A.H. and U.L.A. acknowledge support from the Danish Research Agency (Project No. FTP 274-07-0509) and the EU project COMPAS.

*stm@fotonik.dtu.dk

†pelo@fotonik.dtu.dk;

<http://www.fotonik.dtu.dk/quantumphotonics>

- [1] M. C. W. van Rossum and T. M. Nieuwenhuizen, Rev. Mod. Phys. **71**, 313 (1999).
- [2] S. Hughes, L. Ramunno, J. F. Young, and J. E. Sipe, Phys. Rev. Lett. **94**, 033903 (2005).
- [3] S. I. Bozhevolnyi, V. S. Volkov, and K. Leosson, Phys. Rev. Lett. **89**, 186801 (2002).
- [4] A. L. Moustakas *et al.*, Science **287**, 287 (2000).
- [5] F. Scheffold and G. Maret, Phys. Rev. Lett. **81**, 5800 (1998).
- [6] M. P. van Albada, J. F. de Boer, and A. Lagendijk, Phys. Rev. Lett. **64**, 2787 (1990).
- [7] C. W. J. Beenakker, Phys. Rev. Lett. **81**, 1829 (1998).
- [8] J. Tworzydło and C. W. J. Beenakker, Phys. Rev. Lett. **89**, 043902 (2002).
- [9] P. Lodahl, A. P. Mosk, and A. Lagendijk, Phys. Rev. Lett. **95**, 173901 (2005).
- [10] P. Lodahl and A. Lagendijk, Phys. Rev. Lett. **94**, 153905 (2005).
- [11] S. Balog, P. Zakharov, F. Scheffold, and S. E. Skipetrov, Phys. Rev. Lett. **97**, 103901 (2006).
- [12] P. Lodahl, Opt. Express **14**, 6919 (2006).
- [13] S. E. Skipetrov, Phys. Rev. A **75**, 053808 (2007).
- [14] The spatial quantum correlation function introduced here differs slightly from the one of Ref. [9]. Both definitions contain the same physics in the diffusive regime of consideration here, while they differ in the mesoscopic regime.
- [15] E. Knill, R. Laflamme, and G. J. Milburn, Nature (London) **409**, 46 (2001).
- [16] J. Gómez Rivas *et al.*, Europhys. Lett. **48**, 22 (1999).
- [17] S. Smolka and P. Lodahl (to be published).
- [18] L. A. Wu, H. J. Kimble, J. L. Hall, and H. Wu, Phys. Rev. Lett. **57**, 2520 (1986).
- [19] D. J. Pine, D. A. Weitz, P. M. Chaikin, and E. Herbolzheimer, Phys. Rev. Lett. **60**, 1134 (1988).